Continental Shelf Research 31 (2011) 202–215

Contents lists available at ScienceDirect

Continental Shelf Research

journal homepage: www.elsevier.com/locate/csr

Research papers

Seasonal variability of primary production in a fjord ecosystem of the Chilean Patagonia: Implications for the transfer of carbon within pelagic food webs

Paulina Montero [a,c,f,*], Giovanni Daneri [a,c,f], Humberto E. González [a,c,d,f], Jose Luis Iriarte [a,c,e,f], Fabián J. Tapia [c], Lorena Lizárraga [b,c], Nicolas Sanchez [c,d], Oscar Pizarro [c,f]

[a] Centro de Investigación en Ecosistemas de la Patagonia (CIEP), Bilbao 449, Coyhaique, Chile
[b] Centro de Ciencias y Ecología Aplicada (CEA), Universidad del Mar, Carmen 446, Cerro Placeres, Valparaíso, Chile
[c] Centro de Investigación Oceanográfica en el Pacífico Sur-Oriental (COPAS), Universidad de Concepción, Casilla 160-C, Concepción, Chile
[d] Instituto de Biología Marina, Universidad Austral de Chile, Casilla 567, Valdivia, Chile
[e] Instituto de Acuicultura, Universidad Austral de Chile, Puerto Montt, Chile
[f] Programa COPAS Sur-Austral, Universidad de Concepción, Centro de Investigación en Ecosistemas de la Patagonia, Chile

ARTICLE INFO

Article history:
Received 17 December 2009
Received in revised form
1 September 2010
Accepted 2 September 2010
Available online 29 September 2010

Keywords:
Primary production
Bacterioplankton production
Carbon transfer
Chilean fjord ecosystem

ABSTRACT

We characterized the seasonal cycle of productivity in Reloncaví Fjord (41°30′S), Chilean Patagonia. Seasonal surveys that included measurements of gross primary production, community respiration, bacterioplankton secondary production, and sedimentation rates along the fjord were combined with continuous records of water-column temperature variability and wind forcing, as well as satellite-derived data on regional patterns of wind stress, sea surface temperatures, and surface chlorophyll concentrations. The hydrography and perhaps fjord productivity respond to the timing and intensity of wind forcing over a larger region. Seasonal changes in the direction and intensity of winds, along with a late-winter improvement in light conditions, may determine the timing of phytoplankton blooms and potentially modulate productivity cycles in the region.

Depth-integrated gross primary production estimates were higher (0.4–3.8 g C m^{-2} d^{-1}) in the productive season (October, February, and May), and lower (0.1–0.2 g C m^{-2} d^{-1}) in the non-productive season (August). These seasonal changes were also reflected in community respiration and bacterioplankton production rates, which ranged, respectively, from 0.3 to 4.8 g C m^{-2} d^{-1} and 0.05 to 0.4 g C m^{-2} d^{-1} during the productive and non-productive seasons and from 0.05 to 0.6 g C m^{-2} d^{-1} and 0.05 to 0.2 g C m^{-2} d^{-1} during the same two periods. We found a strong, significant correlation between gross primary production and community respiration (Spearman, $r=0.95$; $p<0.001$; $n=12$), which suggests a high degree of coupling between the synthesis of organic matter and its usage by the planktonic community. Similarly, strong correlations were found between bacterioplankton secondary production and both gross primary production (Spearman, $r=0.7$, $p<0.05$, $n=9$) and community respiration (Spearman, $r=0.8$, $p<0.05$, $n=9$), indicating that bacterioplankton may be processing an important fraction (8–59%) of the organic matter produced by phytoplankton in Reloncaví Fjord. In winter, bacterial carbon utilization as a percentage of gross primary production was >100%, suggesting the use of allochthonous carbon sources by bacterioplankton when the levels of gross primary production are low. Low primary production rates were associated with a greater contribution of small cells to autotrophic biomass, highlighting the importance of small-sized plankton and bacteria for carbon cycling and fluxes during the less productive winter months. Fecal pellet sedimentation was minimal during this period, also suggesting that most of the locally produced organic carbon is recycled within the microbial loop. During the productive season, on the other hand, the area exhibited a great potential to export organic matter, be it to higher trophic levels or vertically towards the bottom.

1. Introduction

Fjords and estuaries play an important role in biological productivity and carbon cycling within aquatic ecosystems (Burrell, 1988; González et al., this issue). These systems receive large contributions of particulate and dissolved organic matter

* Corresponding author at: Centro de Investigación en Ecosistemas de la Patagonia (CIEP), Bilbao 449, Coyhaique, Chile. Tel.: +56 67 244 500; fax: +56 67 244 501.
E-mail address: pmontero@ciep.cl (P. Montero).

0278-4343/$ - see front matter © 2010 Elsevier Ltd. All rights reserved.
doi:10.1016/j.csr.2010.09.003

from both autochthonous (planktonic productivity) and allochthonous sources (detritus from terrestrial plants, urban, and aquaculture waste) that are transported by rivers and surface run-off (Rojas and Silva, 2005). The oceanography of the Chilean Patagonia fjord areas is determined by the interaction of a freshwater influence (coastal run-off) with oceanic Subantarctic Waters (SAAW) driven into the area as the West Wind Drift reaches the southern coast of Chile (Iriarte et al., 2007 and references therein). Besides the estuarine-type circulation set up by the interaction between SAAW and freshwater run-off, the area is characterized by the occurrence of strong diurnal tidal currents.

The general pattern of phytoplankton succession in southern Chile's fjords and channels shows predominantly small flagellates (size range: 2–20 μm) in winter (Czypionka et al., this issue) and a conspicuous diatom bloom in spring, followed by increased abundances of thecate dinoflagellates in summer (Iriarte and Gonzalez, 2008). Although maximum rates of primary production in the surface waters of southern Chile (41–43°S) have been observed mainly in early spring (Iriarte et al., 2007), the phytoplankton biomass in certain areas, such as the Chiloe Interior Sea, remain relatively high over the entire austral summer and early fall (September through May).

The productivity cycle in the Chilean Patagonian fjord and channel areas can thus be divided into productive (late winter/early spring to late fall) and non-productive (winter) seasons. During the productive season, the nutrient supply to the well-lit surface layers becomes the main limitation to phytoplankton primary production and phytoplankton biomass (Pizarro et al., 2000; Iriarte et al., 2007). The hydrodynamic mechanism that usually controls total phytoplankton production is the alternation, in time and/or space, between the destabilization and re-stratification of the water column (Legendre and Razzoulzadegan, 1996). In this context, a prolonged productive season may be taken as an indicator of persistent, hydrodynamically favorable conditions that are fundamental to the overall productivity of fjord areas.

Iriarte and Gonzalez (2008) have suggested that an improvement in the light regime towards the end of winter is the main factor triggering phytoplankton production in the southern Pacific coastal area. It is not clear, however, if this seasonal improvement in light alone is sufficient to trigger the phytoplankton blooms observed in early spring in the fjords of occidental Patagonia. A recent study in the Strait of Georgia, British Columbia (Collins et al., 2009), suggests that wind forcing may have a stronger influence on the timing of the spring phytoplankton bloom than seasonal increases in solar radiation. The interplay between wind-forced vertical mixing, solar radiation, and nutrient availability determines whether the mixed layer is above or below the critical depth and, hence, the occurrence of phytoplankton blooms (Sverdrup, 1953).

Several of the various pathways by which organic carbon is transferred through the food web are known to be determined by the size structure of primary producers and by grazing pressure (Legendre and Razzoulzadegan, 1996). Although there is a number of alternate routes for the transfer of energy (Legendre and Razzoulzadegan, 1995; Legendre and Rivkin, 2002), increasing evidence suggests that microbial (Calbet and Landry, 2004) and/or multivorous food webs (Vargas et al., 2008) are permanent routes for primary production in a variety of ecosystems, in which the microbial and herbivorous grazing modes are equally important for carbon export.

Several authors have argued that bacterioplankton (defined here as a group containing both bacteria and archaea) respond rapidly to increments in primary production and may process a substantial fraction of the organic carbon produced by phytoplankton (Cole et al., 1988; McManus and Peterson, 1988; Williams, 1998; Aristegui and Harrison, 2002; Cuevas et al., 2004; Montero et al., 2007). The microbial heterotrophic community sets an upper limit for the transfer of organic matter to large metazoans and substantially modifies the total amount of organic carbon that can be exported from the euphotic zone (Legendre and Rivkin, 2002, 2008). The strong correlation between rates of gross primary production (GPP), community respiration (CR), and bacterioplankton secondary production (BSP) reflects a significant degree of coupling between the formation of organic matter and its utilization by the microbial heterotrophic community (Montero et al., 2007). Weak coupling between phytoplankton and bacterial production, on the other hand, can be observed when bacterial growth depends on allochthonous organic substrates (Bukaveckas et al., 2002) or when there is a tight top-down control of bacterial populations by their predators (Duarte et al., 2005). Allochthonous organic matter from terrestrial sources may supply labile organic compounds (Newell and Christian, 1981; Button, 1984), which may maintain considerable levels of bacterioplankton production during months of low in situ primary productivity (Albright and McCrae, 1987).

In this study, we document and characterize the seasonal cycle of productivity in Reloncaví Fjord (41.5°S; 72.5°W), southern Chile. Using in situ and satellite-derived data, we first describe the regime of physical variability in the region and its manifestation on local scales. Through concurrent measurements of GPP, CR, BSP, sedimentation rates, and the community structure of phytoplankton, we were able to assess the main carbon fluxes and pathways for organic matter in the study area during periods with contrasting productivity. We also discuss the role of regional and local regimes of wind variability as major drivers of productivity cycles in the Patagonian fjord ecosystems.

2. Materials and methods

2.1. Study area

The study area corresponds to Reloncaví Fjord (41°S; 72°W) (Fig. 1), which receives freshwater inputs from three rivers (Puelo, Petrohué, Cochamó, see Fig. 1) and from several more diffuse sources of freshwater run-off. These inputs interact with the oceanic influence, imposing estuarine-type circulation, with a surface freshwater flow coming from the continent and Subantarctic Waters (SAAW, 31–33 psu) below 20 to 30 m (Silva et al., 1997, 1998). Freshwater from the continent is high in silicate, whereas SAAW possesses high nitrate and phosphate concentrations (Silva, 2008). High loads of fine sediment particles in the freshwater layer limit light penetration to 5 m ($\pm$0.8) in winter and 7 m ($\pm$2.4) in the summer, thereby reducing the available light potential associated with the seasonal increase in solar radiation.

Intensive observations (2–3 consecutive days) were carried out in August 2008 (austral winter), October 2008 (spring), February 2009 (summer), and May 2009 (autumn). Experiments were conducted using a Zodiac boat at three sampling stations located at the mouth (P1, ~100 m of depth), center (P2, ~200 m of depth), and head of the fjord (P3, ~300 m of depth) (Fig. 1). Additionally, in November 2008, total and fractionated chlorophyll-*a* measurements were undertaken along Reloncavi Fjord on board the R/V *Vidal Gormaz*.

2.2. Hydrography and environmental variability

Water column temperature, salinity, and dissolved oxygen were routinely measured on each sampling day using an Ocean Seven 304 CTD (IDRONAUT, Italy). Discrete samples for water

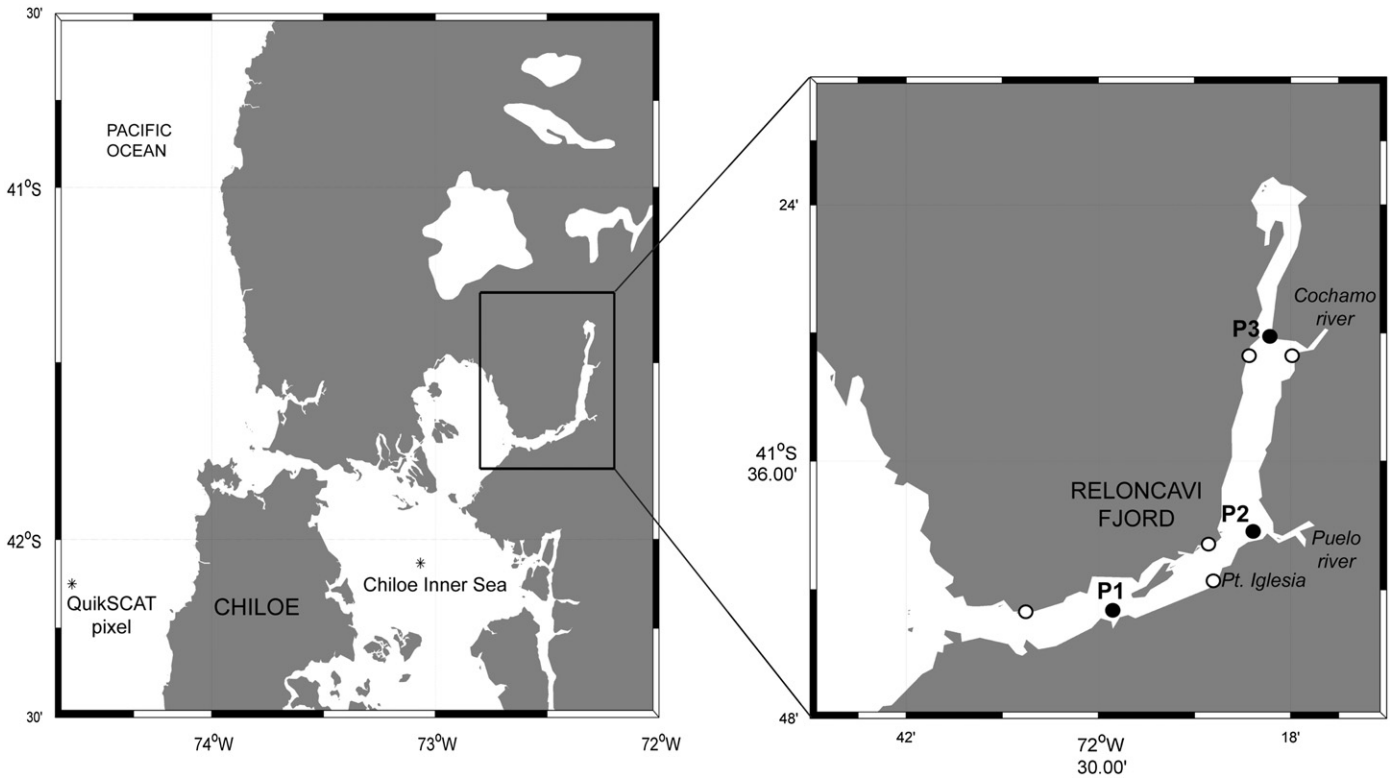

Fig. 1. Regional context and geographic location of Reloncavi Fjord. Black circles indicate sampling stations (P1, P2 and P3) and white circles the position of thermistor moorings installed in August–November 2008 (see Methods).

column variables analyses (see below) were collected on each CTD cast using a Niskin bottle (30 L) from four standard depths (1, 5, 10, 20 m).

Variability in the thermal structure of the water column along the fjord was continuously monitored from August to November 2008, by means of five thermistor lines (see Fig. 1) moored at an average depth of 50 m near the fjord mouth (1 line), southeast of the Puelo river mouth (2 lines), and near the fjord head in the area of Cochamó (2 lines). All moorings consisted of 13 HOBO Pro v2 loggers (Onset Computer Corp.) spaced every 1 m from the surface to 5 m depth, every 2 m from 7 to 13 m depth, and every 5 m from 15 to 25 m depth. Instantaneous water temperature measurements were recorded every 5 min.

The variability of wind forcing during the same period was monitored on both local and regional scales using a meteorological station installed at Punta Iglesia (41°40′S 72°22′W) and QuikSCAT wind fields, respectively. Wind velocities measured at Punta Iglesia were rotated and aligned with their major axis of variability (77° east of true north), which was roughly parallel to the fjord's axis in that area, and then decomposed into their along-fjord (v) and cross-fjord (u)components. Level 3 QuikSCAT data were used to obtain a daily series of wind stress for a pixel located 47 km off the coast of Chiloe and ca. 170 km SW of the Reloncavi Fjord mouth (42°7.5′S, 74°37.5′W). This pixel was chosen based on a compromise between data quality (valid data for $>80\%$ of available L3 images) and distance to our study area. Although we acknowledge that wind variability patterns may change greatly over ca. 170 km of complex topography, we used this satellite-derived record to characterize lower-frequency changes in alongshore wind forcing, namely its seasonal transition from predominately polewards in autumn-winter months (May through September) to equatorwards in spring-summer (October through April), and to compare the timing of such transition with that observed *in situ* during our study. East and north velocities were rotated according to the axis of maximum wind variability (9° west of true north) and used to compute daily series of meridional (τ_v) and zonal (τ_u) wind stress. Meridional winds derived from QuikSCAT were positively and significantly correlated with those recorded at Pt. Iglesia ($r=0.44$, $p<0.001$).

To provide a regional (and seasonal) context for the variability of physical and biological conditions observed in the fjord, we used Level-3 MODIS-Aqua images with 4 km resolution to obtain weekly fields of sea surface temperature (SST, °C) and surface chlorophyll-*a* concentration (Chl-*a*, mg m^{-3}) gathered over the past seven years for a $\sim$5000-km^2 region that encompasses the inner sea located west and south of the fjord mouth. The area, hereafter referred to as the Chiloe Interior Sea (CIS) and centered at 42°4′S, 73°4′W, was chosen as a compromise, considering the distance to the fjord mouth, coverage, and data quality. Only pixels with $>60\%$ good data from 2002 to 2009 were used to compute spatial means of SST and surface chlorophyll from each weekly image. Time series of SST over the CIS was highly correlated with SST averaged over a smaller area ($\sim$64 km^2) at the fjord's mouth ($r=0.63$, $p<0.001$ for first-differenced series), as well as with the in situ SST record gathered from the thermistor mooring located near the fjord's mouth ($r=0.70$, $p=0.025$ for first-differenced series).

2.3. *In situ* observations of nutrients, phytoplankton, and chlorophyll-*a*

Water samples for nutrient analyses (nitrate, phosphate, silicic acid) were filtered through GF/F filters and frozen at −20 °C until spectrophotometric analysis in the laboratory. Nitrate, phosphate, and silicic acid were determined as in Strickland and Parsons (1968). Samples for phytoplankton cell counts consisted of 300-mL subsamples collected with a Niskin bottle from the same depths indicated for nutrients. Samples were stored in clear plastic bottles, fixed, and preserved in a 1% Lugol iodine solution

(alkaline). From each sample, a 50-mL sub-sample was placed in a sedimentation chamber and allowed to settle for 30 h (Utermöhl, 1958) prior to sorting at 40× under an inverted microscope (Wild M40).

For total Chl-*a* determinations, three 100-mL water samples from each of the same four depths were filtered through MFS glass fiber filters with 0.7-μm nominal pore size. Following filtration, samples were immediately frozen (−20 °C) until later analysis by fluorometry, using 90% v/v acetone for pigment extraction and a Turner Design TD-700 fluorometer according to standard procedures (Parsons et al., 1984). Chlorophyll-*a* size fractionation was performed post-incubation in 3 sequential steps: (1) for the nanoplankton fraction (2.0–20 μm), seawater (100-mL) was pre-filtered using 20-μm Nitex mesh and collected on a 2.0-μm Nuclepore; (2) for the picoplankton fraction (0.7–2.0 μm), seawater (100-mL) was pre-filtered using a 2.0-μm Nuclepore and collected on a 0.7-μm MFS (microfiltration system) glass-fiber filter; (3) for the whole phytoplankton community, 100-mL of seawater was filtered through a 0.7-μm MFS glass-fiber filter. The microphytoplankton fraction was obtained by subtracting the Chlorophyll-*a* estimated in Steps (1) and (2) from total Chl-*a* estimated in Step 3. Discrete-depth estimates of Chl-*a* were integrated down to 10 m, using a polynomial method.

2.4. Primary production and community respiration experiments

In situ GPP and CR incubations were conducted during each of the sampling campaigns in August 2008 (austral winter), October 2008 (spring), February 2009 (summer), and May 2009 (autumn), with a total of 12 experiments. Incubations were performed with water samples obtained from 1, 5, 10, and 20 m depth. Estimations of GPP and CR were based on changes in dissolved oxygen concentrations observed after in situ incubations of light and dark bottles (Strickland, 1960). Water from the Niskin bottles was transferred to gravimetrically calibrated borosilicate bottles with a nominal volume of 125-mL using a silicone tube. Five time-zero bottles, five light bottles, and five dark bottles were used for each incubation depth and attached to a surface-tethered mooring system. Water samples were collected at dawn and were incubated during the whole light period. Time-zero bottles were fixed at the beginning of each experiment. Titration was done using an automatic Metrohom burette (Dosimat plus 865) and by visual end-point detection. The average coefficient of variation for replicate samples was 0.03%. GPP values were converted from oxygen to carbon units using a conservative photosynthetic quotient (PQ) of 1.25. (Williams and Robertson, 1991) and the CR values were converted from oxygen to carbon units using a respiration quotient (RQ) of 1. Discrete-depth estimates of GPP and CR were integrated down to 10 m, which usually corresponded to the 1% light depth using a polynomial method.

2.5. Bacterioplankton secondary production

A total of nine BSP experiments were performed during the sampling campaigns of August 2008 (austral winter), October 2008 (spring), and May 2009 (autumn). Experiments were conducted with the same water samples obtained for in situ GPP and CR incubations. Estimates of BSP were based on the incorporation of L-[^{14}C (U)]-leucine (300 mCi mmol^{-1}, 50 nM final saturating concentration) into proteins (Simon and Azam, 1989). Additionally, during the second and third campaigns, we estimated the incorporation of [methyl-3H]-thymidine (11.3 Ci mmol^{-1}, 20 nM final saturating concentration) into DNA (Fuhrman and Azam, 1982; modified by Wicks and Robarts, 1987).

For both methods, a blank and three samples (10 mL) were taken from each sampling depth. Samples were incubated in triplicate for 1 h. The samples and blank were poisoned with 0.2-μm filtered buffered formaldehyde. All incubations (leucine, thymidine) were stopped by adding cold analytical trichloroacetic acid (TCA) 50% w/v. Samples incubated with the thymidine method were further treated with 5 mL of phenol–chloroform solution (50% w/v) and 5 mL of cold analytical-grade ethanol (80% w/v). After 10 min, the tube contents were filtered (0.22-μm pore size GSWP Millipore). The dried filters were transferred to borosilicate scintillation vials, where they were kept cool until radioisotopic analysis. In the laboratory, the vials were treated with analytical ethyl acetate and 10 mL of liquid scintillate Ecolite (+) (ICN). All samples were measured in dpm using a Packard (Mod. 1600 TR) liquid scintillation counter.

The thymidine uptake was transformed into cell production using a constant of 2×10^{18} cells per mole of thymidine incorporated (Fuhrman and Azam, 1982). Leucine incorporation rates were transformed into bacterial carbon following the rationale of Simon and Azam (1989). BSP was converted to Bacterial Carbon Utilization (i.e., gross bacterioplankton secondary production using a Bacterial Growth Efficiency estimated as in Rivkin and Legendre (2001). Throughout the text, BSP refers to gross bacterioplankton secondary production. Discrete-depth estimates of BSP were integrated down to 10 m.

2.6. Bacterioplankton, nanoflagellates, and microzooplankton

Water samples for bacterioplankton and nanoflagellates (heterotrophic and autotrophic) counts (50 mL) were collected from the same depths indicated above. Samples were preserved with glutaraldehyde (2% v/v) and kept in the dark at 4 °C until counting by epifluorescence microscopy. Two and three milliliter of seawater containing bacteria were filtered onto 0.2-μm black polycarbonate filters and stained with DAPI (4′6-diamidine 2-phenylindole) to a final concentration of 0.01% w/v, according to Porter and Feig (1980). For nanoflagellates, 20–30 mL were filtered onto 0.8-μm black polycarbonate filters and stained with Proflavine (3-6-diamidine-acridine hemi-sulfate) to a final concentration of 0.033% w/v, according to Hass (1982). Estimates of bacterioplankton and nanoflagellate biomass were obtained using conversion factors of 20 (Lee and Fuhrman, 1987) and 6500 fgC cell^{-1} (Børsheim and Bratbak, 1987), respectively.

Concentrated samples (100 mL) for microzooplankton analyses were obtained by filtrating 7 to 18 L of seawater through a 20-μm mesh and preserving this with an acidified Lugol solution (1%) until microscopic enumeration (Utermöhl, 1958) by inverted microscopy (Zeiss Axiovert phase contrast). Biovolume was estimated according Sun and Liu (2003). Biomass was calculated from biovolume estimates using the equations: pgC=(μm^3)∗0.053+444.5 (Verity and Langdon, 1984) and pgC=(μm^3)∗0.13 (Edler, 1979) for ciliates and dinoflagellates, respectively. Discrete-depth estimates of biomass were integrated down to 10 m.

2.7. Flux of particulate material

To characterize and quantify the flux of particulate material to the fjord bottom, sediment traps with a collection area of 198.94 cm^2 were installed at 50 m depth for 2 to 3 days during each campaign. At the end of each period, collected samples were preserved with a 1% acidified Lugol solution. We estimated the vertical carbon flux associated with diatoms, microzooplankton, and fecal pellets. The vertical flux of planktonic organisms was expressed in cells m^{-2} d^{-1}. Biovolume was estimated according to Sun and Liu (2003) and used to calculate the biomass of

diatoms as pgC=(μm^3)*0.13 (Edler, 1979). The volume of fecal pellets was converted to biomass according to González et al., (2000), where 1 mm^{-3} of fecal pellet =0.07617 mgC. Biovolume-to-biomass conversions for microzooplankton were done using pgC=(μm^3)*0.053+444.5 (Verity and Langdon, 1984) for ciliates and pgC=(μm^3)*0.13 (Edler, 1979) for dinoflagellates. Prior to gravimetric analyses, samples were divided equally into pre-combusted and pre-weighted filters ($\pm$0.00001 g) to obtain the total dry weight (seston) and, after 5 h of muffle combustion at 550 °C, the lithogenic fraction (inorganic). The weight of organic matter in the samples was estimated by subtracting these two measurements.

3. Results

3.1. Physical variability: in situ meteorological variables and satellite-derived SST, Chl-a, and wind data

Meteorological observations gathered at Punta Iglesia in winter and spring 2008 showed a marked transition in the regime of wind forcing and precipitation in the fjord (Fig. 2). A cumulative plot of along-fjord wind velocities indicated that the sudden change in wind forcing took place on 9 September, when the dominant frequencies of wind variability switched from synoptic to diurnal (results not shown). This shift in the variability of local winds appeared to track larger-scale changes in atmospheric forcing, as suggested by a dramatic change in meridional winds measured by QuikSCAT off Chiloé Island (see Fig. 3). After four months of intense, persistent, poleward winds, a sudden relaxation of meridional winds occurred around 1 September 2008 (Fig. 3) and lasted for ca. 3 months. Similarly, strong or stronger poleward winds were recorded in winter 2002 and 2006 (Fig. 4A).

Our inspection of satellite-derived data on the variability of coastal winds, SST, and surface Chl-*a* over the past seven years indicated that poleward winds were dominant in the fall-winter months, whereas the spring-summer months were characterized by equatorward winds interspersed with periods of relaxation and/or reversal (Fig. 4A). Surface chlorophyll concentrations over the Chiloe Interior Sea (Fig. 4B) increased in late winter-early spring (late August-early September) and remained high until mid-fall (May of the following year), thereby defining two contrasting periods for primary production: the productive period (September to May; Chl-*a* >5 mg m^{-3}) and the non-productive period (May to August; Chl-*a* <1 mg m^{-3}). A clear annual cycle was detected in SST as well (Fig. 4B), with maximum (minimum) temperatures in February (July–August) and annual ranges 5–6 °C. This annual SST cycle was consistent with the annual change in solar radiation documented for the area by Iriarte and Gonzalez (2008) and did not appear to be affected by inter-annual changes in the intensity of wind forcing.

3.2. Continuous temperature profiles and nutrient concentrations

The shift in atmospheric forcing observed in September 2008 was followed by a rapid change in the thermal structure of the fjord's water column. This dramatic, persistent change was apparent from continuous records of temperature profiles gathered at five points along the fjord and took place around 15 September, when the 10 °C isotherm intersected the surface and the surface-to-bottom temperature difference switched from <-1.5 to >1.5 °C (Fig. 5). Prior to this shift, which was coherent throughout the fjord (Fig. 5A–E), temperatures below the surface layer were slightly greater than 10 °C and fairly homogenous. These values were consistent with temperatures measured in the deeper layers (from ca. 20 to 200 m depth) all year round.

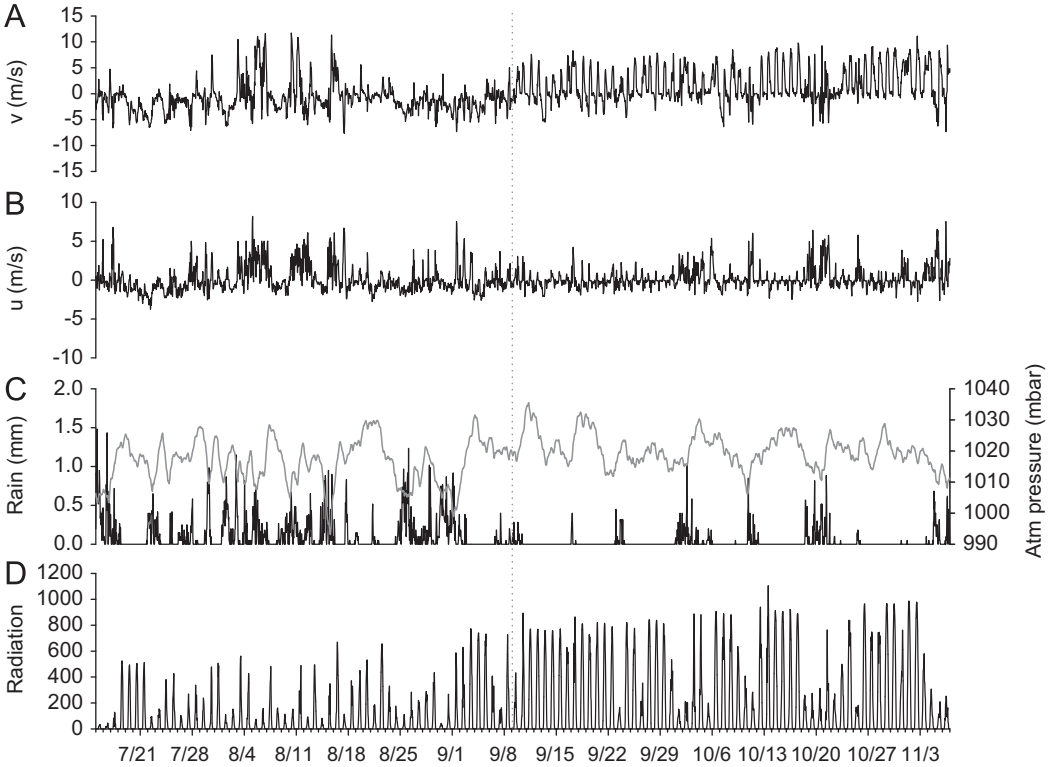

Fig. 2. Hourly time-series of meteorological variables measured at Punta Iglesia (41°40′S 72°22′W, see Fig. 1) in winter and spring 2008: along-fjord (A) and across-fjord (B) components of wind velocity, atmospheric pressure (C, gray line), precipitation (C, black line), and solar radiation (D). Components of wind velocity were calculated relative to the main axis of variability, which lay at 77° east of true north. The dotted vertical line indicates the day on which a change in the pattern of wind forcing was detected (9 September).

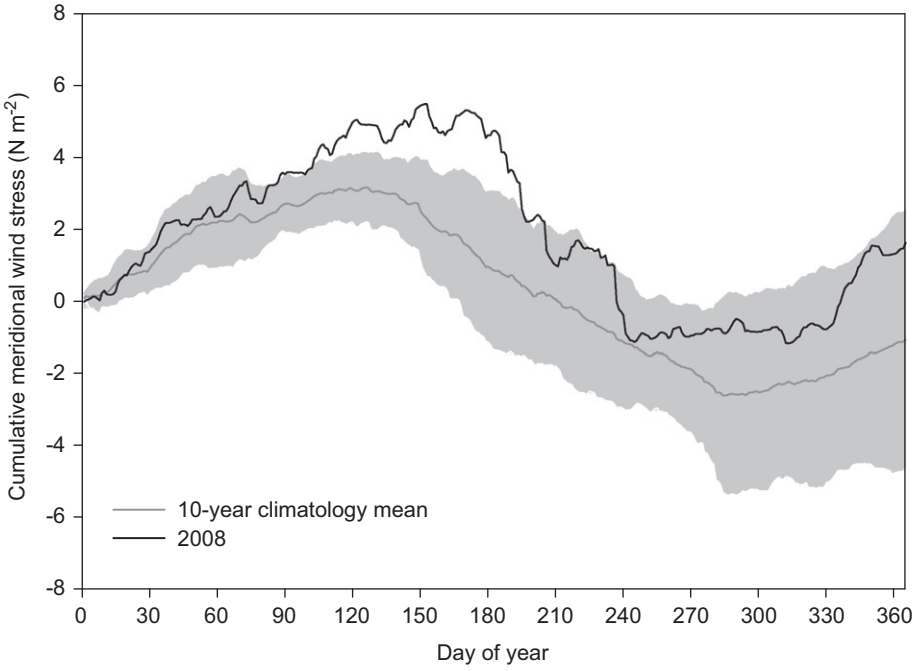

Fig. 3. Cumulative meridional wind stress recorded during 2008 (black line), superimposed on a 10-year climatology computed from available QuikSCAT data for a coastal pixel centered at 42°7.5′S, 74°37.5′W and located off the west coast of Chiloe (see Fig. 1). Shaded area corresponds to 1 standard deviation around the mean (gray line).

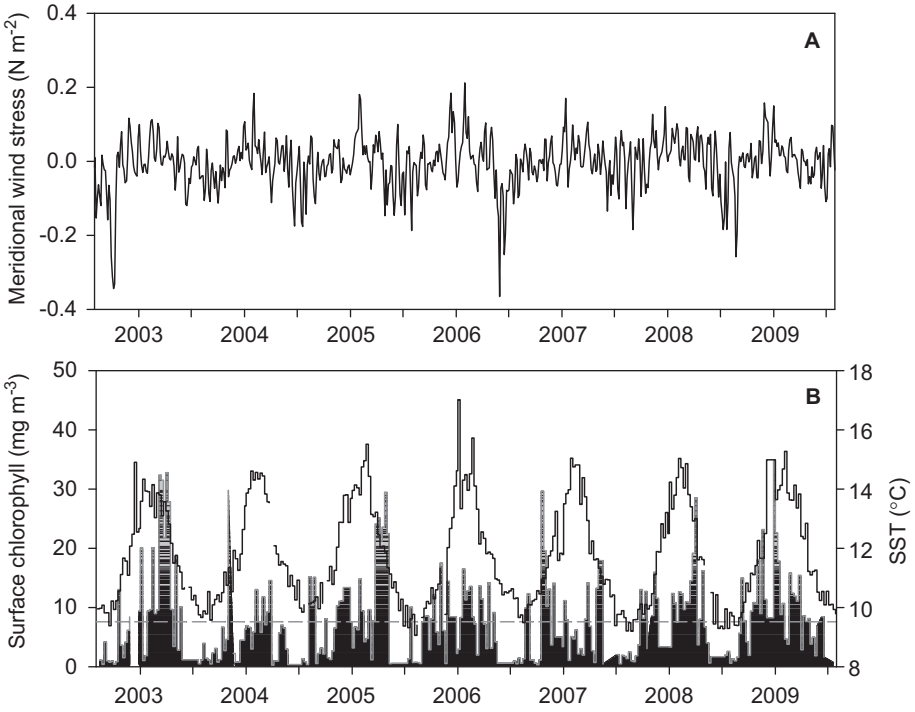

Fig. 4. Satellite-derived time series of (A) daily meridional wind stress from a coastal QuikSCAT pixel centered at 42°7.5′S, 74°37.5′W (see Fig. 1), and (B) spatial means of SST (lines) and surface chlorophyll (bars) derived from weekly MODIS composite images for a region centered at 42°4′S, 73°4′W in the Chiloe Interior Sea (see Methods). The dashed gray line corresponds to the long-term mean chlorophyll concentration (7.58 mg m^{-3}).

CTD profiles gathered during our sampling campaigns showed marked seasonal changes in thermal and saline structures and a dominance of salinity over temperature as the main variable driving water-column stratification (Fig. 6). Whereas surface temperatures reached their maximum (minimum) values of ~18 °C (~10 °C) in February (minimum value in August), the surface layer of freshwater reached its maximum thickness in winter-spring (minimum value in austral autumn) (Fig. 6). In August 2008 (winter) and May 2009 (autumn), a greater input of cold and fresh (< 10 psu) surface waters resulted in a thermal inversion within the top 10 m (Fig. 6). Below the top layer, salinity fluctuated between 30 and ~33 psu. The lowest salinities were always measured towards the fjord head (St. P2 and P3, Fig. 1) and were associated with higher oxygen levels (Fig. 6). Maximum oxygen concentrations (> 10 mg/L) were recorded in the top layer during the spring campaign (October 2008).

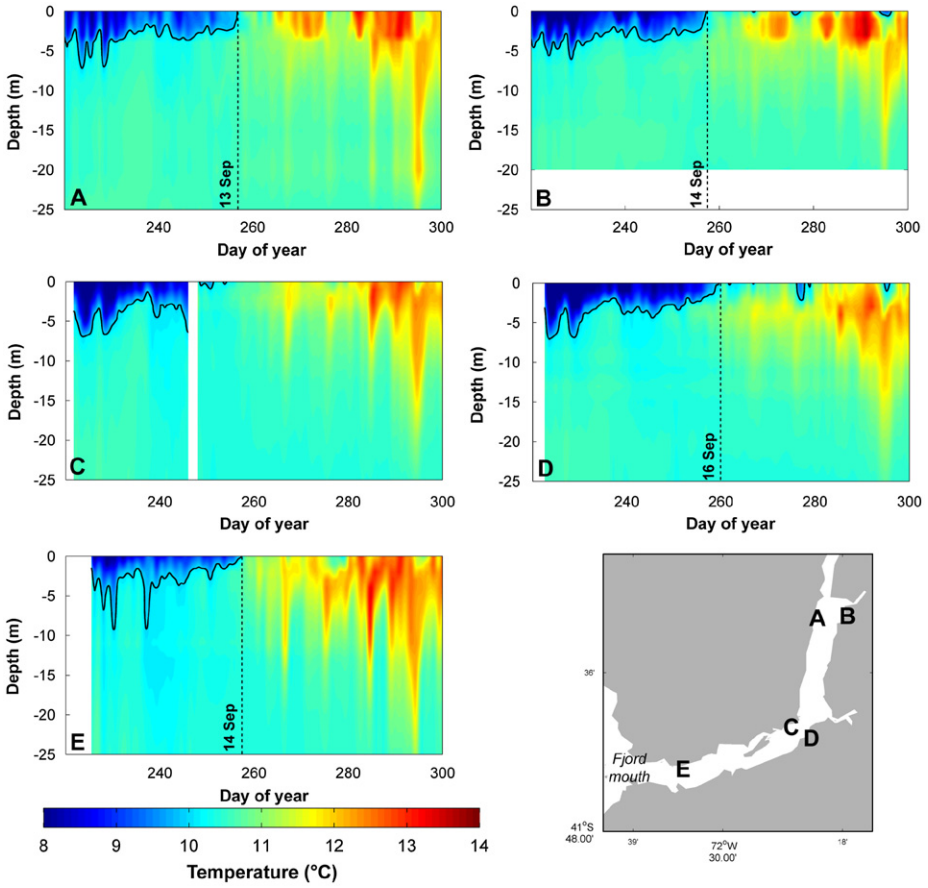

Fig. 5. Temporal variability of thermal structure recorded at five points along the fjord in August–November 2008. The black contour corresponds to 10 °C. Dotted vertical lines indicate the day on which the 10 °C isotherm reached the surface.

Nutrient concentrations exhibited distinct vertical and seasonal patterns of variability (Table 1). Surface concentrations of nitrate and phosphate were high in winter and low in spring (Table 1). Spring concentrations of these nutrients at 10 m depth were consistently higher than those measured at 1 and 5 m, whereas spring silicic acid concentrations always reached their maxima at the surface, in association with low salinities (Table 1). This winter-spring drop in surface nutrient concentrations was consistent with the observed increase in primary production rates (see below). Significant negative correlations were found between GPP values and concentrations of $NO_3^-$and PO_4^{-3} (Table 4) measured during our campaigns, indicating that algal activity is the main factor influencing the seasonal drop in water column nutrient concentrations.

3.3. Gross primary production and community respiration

Estimates of GPP showed marked seasonality, with the highest integrated GPP rates in October 2008 and February and May 2009 (0.4–3.8 g C m^{-2} d^{-1}) and the lowest values in August 2008 (0.1–0.2 g C m^{-2} d^{-1}). During the productive period GPP was always maximum towards the fjord head (i.e., at St. P2 and P3), highlighting the relevance of more sheltered areas for the overall productivity of the fjord ecosystem (Fig. 7). Estimates of CR also showed a seasonal pattern, with the lowest and highest values during the non-productive (0.05–0.40 g C m^{-2} d^{-1}) and productive seasons (0.33–4.79 g C m^{-2} d^{-1}), respectively. The maximum GPP and CR values were observed in February 2009 (Fig. 7). Estimates obtained for these two rates during our study were significantly correlated (Table 4).

The GPP/CR ratio, used as an index for the trophic status of the system, ranged from 0.5 to 2 (Fig. 7), with most experiments indicating an autotrophic metabolism (GPP/CR >1). Throughout the study period, only St. P1 (near the fjord mouth) showed seasonal changes in GPP/CR ratios, being autotrophic during the productive season and heterotrophic during the non-productive season. Station P2 always showed an autotrophic metabolism (GPP/CR >1), whereas heterotrophic processes dominated (GPP/CR <1) at St. P3 (Fig. 7).

3.4. Chlorophyll-a and phytoplankton community

The highest and lowest values of depth-integrated Chl-*a* were observed in February 2009 (productive season, 20–45 mg m^{-2}) and August 2008 (non-productive season, 4–9 mg m^{-2}) (Table 2). Depth-integrated Chl-*a* and GPP were positively and significantly correlated (Table 4). The contribution to total Chl-*a* of the three phytoplankton size fractions (<2 μm, 2–20 μm, >20 μm) revealed a dominance of picophytoplankton (<2 μm) during surveys conducted in August, October, and November 2008, and a greater contribution of microphytoplankton (>20 μm) during the intensive samplings of February and May 2009 (Fig. 8A).

The biomass normalized productivity (GPP/Chl-*a*) was higher during October 2008 and February 2009 (range 50–195) and lower during August 2008 and May 2009 (range 11–47).

The microphytoplankton community showed a marked seasonal pattern (Fig. 8B). The highest and lowest values of depth-integrated phytoplankton abundance were observed in October 2008 (spring, 240,000–431,000 $\times 10^6$ cell m^{-2}) and August 2008 (winter, 500–1200 $\times 10^9$ cell m^{-2}) (Fig. 8B). The main

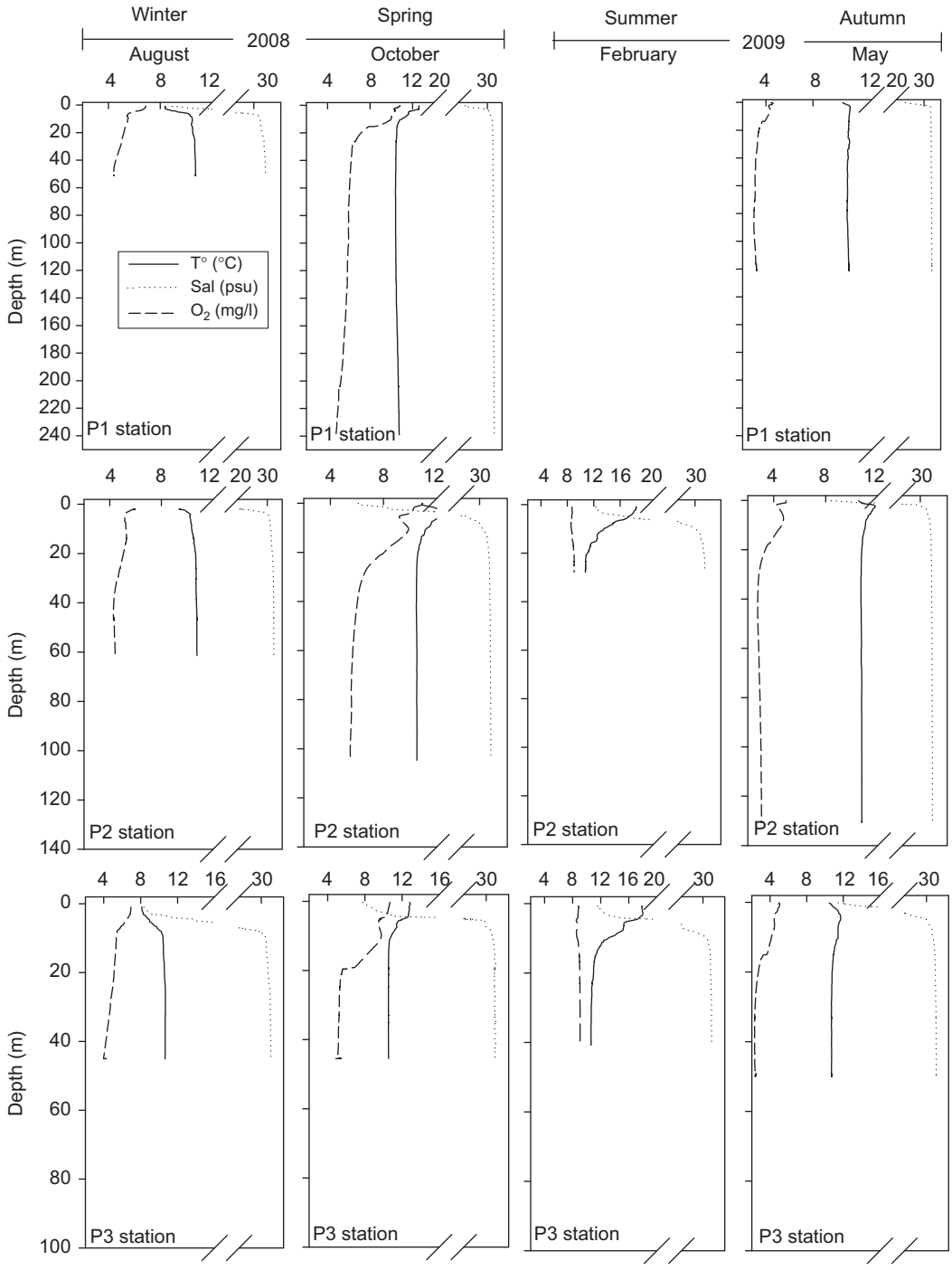

Fig. 6. Temporal and vertical distribution of the hydrographic variables during the study period.

contribution to microphytoplankton abundance corresponded to diatoms of genus *Skeletonema*, which accounted for over 70% of the total abundance in August–October 2008 and May 2009 (Fig. 8B). In February 2009, a large fraction of the microphytoplankton community corresponded to thecate dinoflagellates (Dinophyceae), which were mainly represented ($>60\%$) by the mixotrophic dinoflagellate *Prorocentrum micans* (Fig. 8B). A weak correlation was found between depth-integrated microphytoplankton abundance and GPP values during the study period (Table 4). This result was heavily influenced by the summer (February 2009) data. The exclusion of the February 2009 values resulted in a highly significant correlation (Table 4).

3.5. Bacterioplankton secondary production, gross primary production, and community respiration

Estimated rates of BSP ranged between 0.05 and 0.6 g C m^{-2} d^{-1} (Fig. 9, Table 2). Although leucine-based estimates of BSP did not show consistent seasonal differences throughout the fjord, thymidine-based estimates showed dramatic differences between October 2008 and May 2009 at all three stations (Fig. 9). Both methods for estimating BSP yielded similar rates in May 2009. On the contrary, in October 2008, thymidine-based BSP was twice as high as leucine-based BSP. Higher BSP estimates (both methods) were always obtained at St. P3 near the fjord head (Fig. 9).

Table 1
Nutrient concentrations measured at three stations (P1, P2, P3) along the Reloncavi Fjord in winter-spring 2008 and autumn 2009. Numbers in parentheses correspond to standard deviations.

	Depth (m)	**Winter 2008**						**Spring 2008**						**Autumn 2009**			
		12 Aug **P1**		9 Aug **P2**		13 Aug **P3**		14 Oct **P1**		16 Oct **P2**		15 Oct **P3**		13 May **P1**		14 May **P2**	12 May **P3**
Nitrate (μM)	1	–	–	23.64	(0.03)	9.56	(0.00)	0.60	(0.01)	0.50	(0.02)	0.40	(0.03)	6.76	(0.00)	–	–
	5	13.96	(1.28)	6.61	(0.01)	5.58	(0.10)	3.00	(0.04)	0.90	(0.10)	–	–	6.87	(0.00)	–	–
	10	18.75	(0.58)	16.05	(0.20)	15.47	(0.02)	5.60	(0.30)	7.50	(0.01)	15.50	(0.20)	7.56	(0.28)	–	–
Phosphate (μM)	1	–	–	2.38	(0.050)	1.16	(0.03)	0.02	(0.003)	0.07	(0.05)	0.03	(0.01)	0.95	(0.000)	0.57(0.01)	0.87(0.01)
	5	1.70	(0.05)	0.85	(0.020)	0.71	(0.01)	0.59	(0.001)	0.08	(0.06)	–	–	1.54	(0.013)	1.85(0.08)	1.37(0.02)
	10	2.09	(0.03)	2.15	(0.004)	1.85	(0.04)	1.85	(0.050)	1.04	(0.03)	2.58	(0.05)	2.57	(0.013)	2.24 (0.03)	2.34(0.00)
Silicic acid (μM)	1	–	–	23.67	(0.40)	84.79	(0.90)	49.60	(0.74)	95.9	(1.33)	23.6	(0.41)	12.88	(0.03)	72.3 (0.00)	178.5(0.28)
	5	39.28	(0.10)	105.57	(0.60)	122.51	(0.20)	3.70	(0.00)	35.8	(0.39)	–	–	22.33	(0.03)	81.5 (0.14)	152.9 (0.28)
	10	25.90	(0.10)	35.28	(0.50)	48.22	(0.05)	18.20	(0.25)	12.6	(0.28)	19.7	(1.36)	21.43	(0.61)	130.5(0.14)	125.6(0.00)

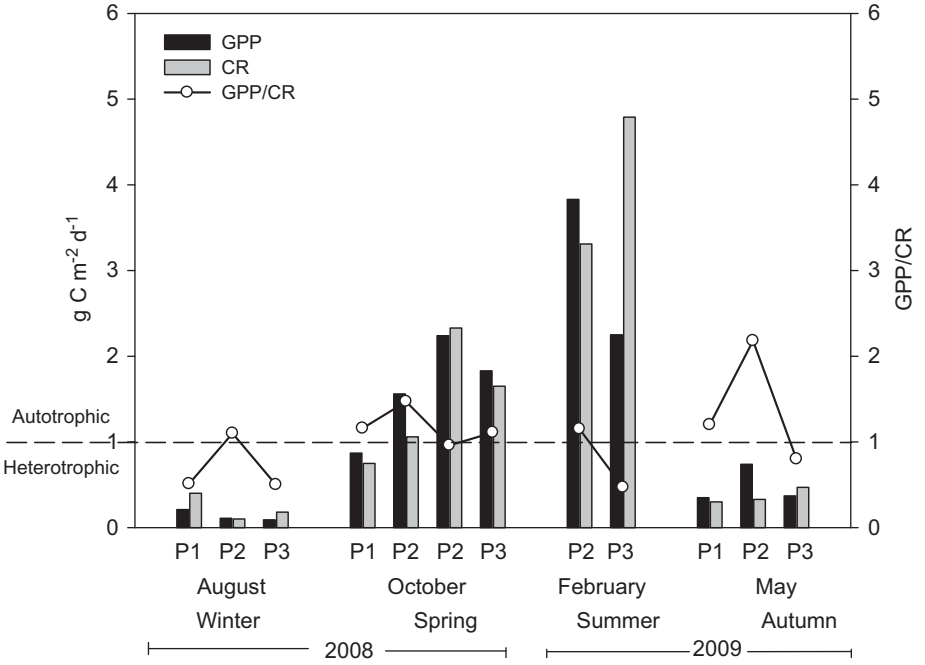

Fig. 7. Gross primary production (GPP), community respiration (CR) and GPP/CR ratio in the study area. The values are integrated over 10 m depth.

Table 2
Estimates of gross primary production, community respiration and bacterioplankton secondary production along the Reloncavi fjord during study period.

Date	Station	Total Chl-*a* mg m^{-2}	GPP g C m^{-2} d^{-1}	CR g C m^{-2} d^{-1}	BSP (leucine) g C m^{-2} d^{-1}	% utilization	BSP (thymidine) g C m^{-2} d^{-1}	% utilization
12-Aug-08	P1	8.6	0.21	0.4	0.05	24	n.d.	n.d.
9-Aug-08	P2	4.3	0.11	0.1	0.16	145	n.d.	n.d.
13-Aug-08	P3	5.1	0.09	0.2	0.17	189	n.d.	n.d.
14-Oct-08	P1	16.8	0.87	0.75	0.19	22	0.40	46
16-Oct-08	P2	18.4	1.56	1.06	0.22	14	0.44	28
17-Oct-08	P2	n.d.	2.24	2.33	n.d.	n.d.	n.d.	n.d.
15-Oct-08	P3	19	1.83	1.65	0.25	14	0.60	33
26-Feb-09	P1	38.4	n.d.	n.d.	n.d.	n.d.	n.d.	n.d.
27-Feb-09	P2	19.7	3.83	3.31	n.d.	n.d.	n.d.	n.d.
28-Feb-09	P3	44.5	2.25	4.79	n.d.	n.d.	n.d.	n.d.
13-May-09	P1	31.6	0.35	0.30	0.05	14	0.05	14
14-May-09	P2	15.8	0.74	0.33	0.09	12	0.06	8
12-May-09	P3	27.3	0.37	0.47	0.22	59	0.16	43

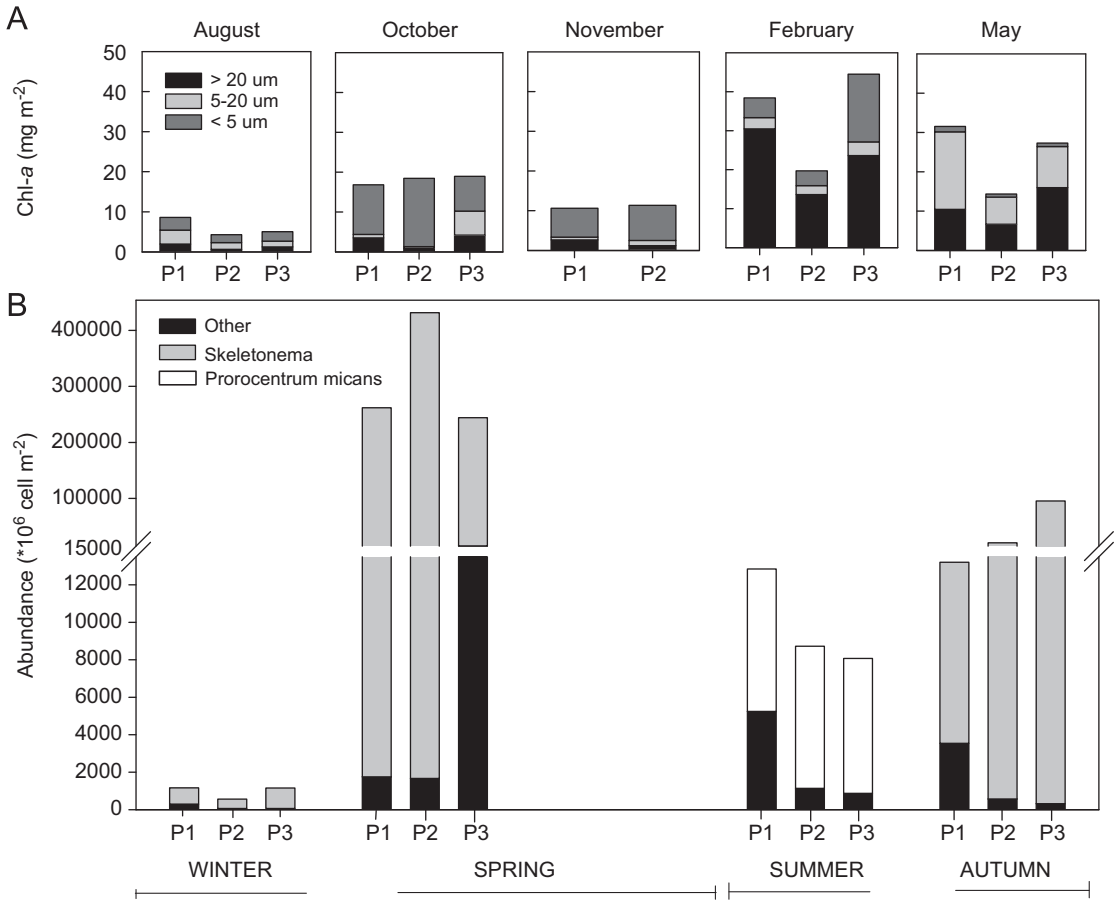

Fig. 8. (A) Contribution to total Chl-*a* of the three phytoplankton size fractions (<2 μm, 2–20 μm, >20 μm). (B) Seasonal abundance of phytoplankton community. The values are integrated over 10 m depth.

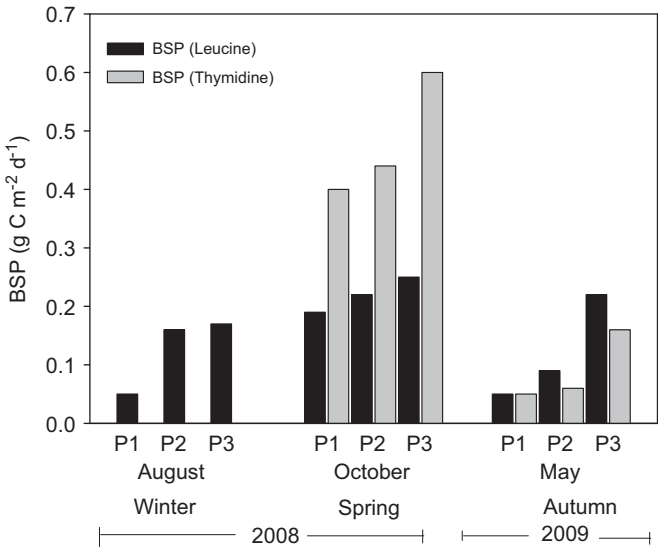

Fig. 9. Bacterioplankton secondary production (BSP). The values are integrated over 10 m depth.

BSP estimates were significantly correlated with GPP and CR rates (Table 4). The percentage of GPP utilized by bacteria ranged from 8% to 189% during the study period. This range was heavily influenced by the leucine-based BSP estimates obtained in August 2008 at St. P2 and P3 (Table 2). The exclusion of these values narrowed the range 8–59% during the productive season.

3.6. Interrelationship between microplanktonic communities

Depth-integrated bacterioplankton biomass (BB) ranged from 66.4 mg C m^{-2} in August 2008 (non-productive season) to 291.5 mg C m^{-2} in February 2009 (productive season, Fig. 10). The distribution of these values did not show clear differences along the fjord. Vertically, biomass was highest within the 5 to 10 m layer. BB was significantly correlated with GPP values (Table 4).

Autotrophic nanoflagellates (ANF) showed the highest values of biomass (211.5 mg C m^{-2}) in February 2009 while the minimum biomass values were observed in May 2009 (1.27 mg C m^{-2}, Fig. 10). ANF and GPP were weakly correlated (Table 4).

The grazer community was composed of heterotrophic nanoflagellates (HNF), dinoflagellates, and ciliates. The highest and lowest abundances of this group were observed in the productive and non-productive seasons (Fig. 10). Like bacterioplankton, these groups responded quickly to increased GPP rates and to the seasonal pattern of Chl-*a* (Table 4). Additionally, dinoflagellates and ciliates were closely coupled with HNF and BB (Table 4). HNF and BB were also significantly correlated (Table 4).

Due to exceedingly high growth rates of dinoflagellates (*Prorocentrum micans*), the grazer biomass exceeded the biomass of bacterioplankton and Chl-*a* in February 2009.

3.7. Flux of particulate material

The flux of particulate material at 50 m exhibited seasonal variations both in composition and magnitude. The lowest and highest estimates for the total flux of material (seston) were

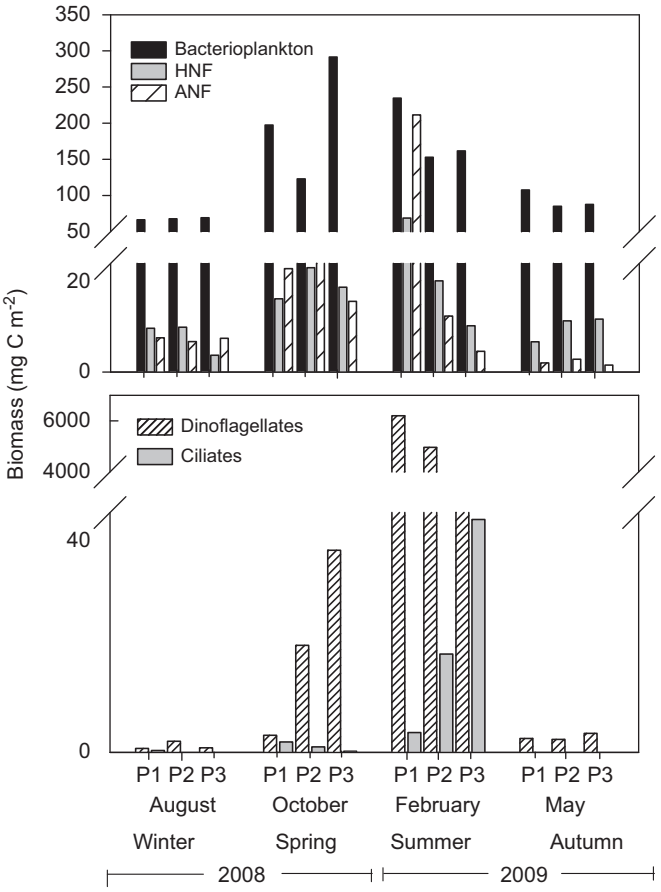

Fig. 10. Biomass of the bacterioplankton and grazer community. The values are integrated over 10 m depth.

Table 3
Flux of particulate material (mg C m^{-2} d^{-1}) during study period in the Reloncavi fjord.

	Winter August 2008	Spring October 2009	Summer February 2009	Autumn May 2009
Total Seston	2676	3239	3759	6150
Lithogenic material	2141	1917	2380	4842
Total organic matter	535	1322	1379	1308
Particulate organic carbon	68	90	n.d.	n.d.
Copepod pellets	0.2	0.4	1.0	2.9
Euphausiids pellets	3.5	9.9	15.0	13.1
Apendicularians pellets	0.9	12.1	3.2	1.5
Undetermined pellets	0.8	0.0	1.2	0.2
Diatoms	0.4	13	0.01	0.8
Microzooplankton	1	0	5	0.2

obtained in August 2008 (2676.4 ± 436.2 mg m^{-2} d^{-1}) and May 2009 (6150.3 ± 38.1 mg m^{-2} d^{-1}), whereas fluxes of total biogenic carbon were highest in October 2008 (35.2 mg m^{-2} d^{-1}) and lowest in August 2008 (non-productive season; 6.3 mg m^{-2} d^{-1}; Table 3). The flux of total biogenic carbon was dominated by fecal pellets, which contributed an average of over 80% of the total carbon flux during the study. Euphausiids and appendicularians provided most of the fecal material (contributing 64% and 24%, of the total, respectively). Copepod pellets and those of undetermined origin represented the remaining 12%.

Table 4
Results of correlation analysis (*Spearman*) between measured variables during study period in the Reloncaví fjord.

Correlated variables	Spearman, *r*	*p*_level	*n*
NO_3^-–GPP	−0.71	0.0006	19
PO_4^{-3}–GPP	−0.63	0.0005	25
$Si(OH)_4$–GPP	0	1	25
Chl-a–GPP	0.64	0.035	11
GPP –CR	0.95	0.000002	12
PA–GPP	0.52	0.082	12
SA–GPP	0.92	0.0005	9
GPP–BSP	0.68	0.042	9
BSP–CR	0.78	0.035	9
GPP–BB	0.82	0.002	11
GPP–HNF	0.4	0.28	11
GPP–GC	0.95	0.000005	11
Chl-a–GC	0.6	0.038	12
HNF–BB	0.82	0.011	12
DC–HNF	0.87	0.00026	12
DC–BB	0.7	0.011	12

GPP, gross primary production; CR, community respiration; BSP, bacterioplankton secondary production; Chl-*a*, Chlorophyll *a*; PA, phytoplankton abundance; *SA*, *Skeletonema sp*. abundance; GC, Grazer community; BB, bacterioplankton biomass; HNF, heterotrophic nanoflagellates; DC, dinofloagellates and ciliates; NO_3^-, nitrate; PO_4^{-3}, phosphate; $Si(OH)_4$, silicic acid.

The total flux of carbon corresponding to diatoms was over one order of magnitude higher in October 2008 (12.8 mg C m^{-2} d^{-1}) than during the other three campaigns (0.01–0.8 mg C m^{-2} d^{-1}; Table 3) and corresponded mainly to *Rhizosolenia* and *Skeletonema*, which accounted for 36% of the total carbon flux (Table 3). The total flux of carbon from microzooplankton, on the other hand, was highest in February 2009 (5 mg C m^{-2} d^{-1}) and up to one order of magnitude lower during the other three campaigns (Table 3). Most of the microzooplankton found during the February 2009 campaign (92%) corresponded to the mixotrophic dinoflagellate *Prorocentrum micans* (54%) and the tintinnids *Dadayella* spp. (38%).

4. Discussion

The southern Chilean fjords are characterized by dramatic seasonal changes in atmospheric conditions (i.e., solar radiation and precipitation; Pickard, 1971; Acha et al., 2004), which exert a strong influence on both biomass and production rates of phytoplankton assemblages. Our analyses of in situ measurements of phytoplankton productivity, biomass, and associated fluxes, together with ancillary satellite data on regional-scale variability of wind forcing and surface chlorophyll, suggest that mesoscale changes in the direction and intensity of winds may modulate the hydrography, productivity cycles, and their inter-annual variability in the fjord and channel ecosystems of the Chilean Patagonia.

Available satellite data on meridional wind stress over the past 10 years have indicated that the strength and persistence of the poleward winds, which prevail in the region in winter, may experience substantial inter-annual variability, as could the timing and duration of the relaxation period (usually in September). Although the productive season in the region (inferred from satellite-derived surface Chl-*a* data) tends to begin and end at about the same time each year (September and May, respectively), surface chlorophyll increased and dropped sharply at variable times within this period. This suggests that the annual solar radiation cycle must interact with mesoscale patterns of wind variability to modulate the productivity of fjord and channel ecosystems in the Chilean Patagonia. We propose that a closer inspection and quantitative modeling of mesoscale wind patterns

and their timing relative to the annual cycle of solar radiation and river run-off (see Collins et al., 2009) may shed light on the complex interactions that determine the timing of phytoplankton blooms in this region. Incorporating data on the annual cycle of photosynthetically available radiation in the area, along with a better understanding of the balance between nutrient inputs from oceanic sources and river run-off into the euphotic zone (see Goebel et al., 2005), may provide us with the necessary tools to model the physical–biological interactions that set the timing of the phytoplankton bloom and the duration of the productive season in Chilean fjords.

Such conclusions would challenge the current perception that the annual cycle of solar radiation is the sole factor triggering phytoplankton blooms in the study region (Iriarte and Gonzalez, 2008). Our results suggest that the patterns observed in the productivity and biomass of phytoplankton assemblages in Reloncavi Fjord may respond, as stated by Collins et al. (2009), to mesoscales changes in the wind pattern in the region. Collins et al. (2009) have shown that, although the seasonal increase in solar radiation is important, the timing of the spring bloom in the Strait of Georgia (British Columbia) is mainly controlled by the interplay between wind stress and water column stratification. Drastic changes in water-column stratification observed during our study, with increased stratification in the productive season, may be the result of mesoscale changes in wind forcing, constituting a key driver of algal blooms within Reloncavi Fjord and similar basins throughout occidental Patagonia.

The hydrographic structure of Reloncaví Fjord is characterized by a surface salinity minimum and silicic acid concentrations maximum, and by temperatures and dissolved oxygen concentrations that peak in austral spring and summer. Within the saline layer, on the other hand, dissolved oxygen concentrations are low, whereas nitrate and phosphate are persistently high. These vertical patterns in hydrography and nutrient concentrations fit the general pattern of seasonal variability previously described for the channels and fjords in southern Chile (Silva et al., 1997, 1998; Silva and Prego, 2002; Silva, 2008), where a silicic acid-rich layer of freshwater lies on top of a saline subsurface layer with high N and P concentrations, and hydrographic properties that are characteristic of open ocean waters (i.e., Subantarctic Surface Water; Chaigneau and Pizarro, 2005). During the productive season and in the absence of persistent hydrodynamic phenomena that force nutrient replenishment in the euphotic zone, the supply of N and P to the well-lit surface layer would be the chief limiting factor for phytoplankton growth (Pizarro et al., 2000; Iriarte et al., 2007). However, an alternation in time and/or space between nutrient replenishment and depletion driven by the destabilization and re-stratification of the water column (Legendre and Razzoulzadegan, 1996) could generate substantial intra-seasonal differences in both planktonic productivity (both in terms of primary production and biomass) and the community structure. Hence, the examination of spatial and/or temporal variability in some of the key parameters estimated during our study may provide an indication of which of the above-described scenarios is a better approximation to Reloncaví Fjord and its functioning.

Estimates of GPP and Chl-*a* obtained during our seasonal surveys agreed well with productivity measurements reported in previous studies for the Chiloé Interior Sea (41.5–43°S; Iriarte et al., 2007) and the Aysén region (43–46°S; Pizarro et al., 2005). During the non-productive season (August 2008), autotrophic biomass and GPP values ranged from 4 to 9 mg m^{-2} and 0.09 to 0.21 g C m^{-2} d^{-1}, respectively, reflecting the low productivity of the system during this period. In contrast, the GPP was substantially higher in October 2008 and February 2009 (up to 3.8 g C m^{-2} d^{-1}), whereas the highest autotrophic biomass was observed in February and May 2009 (16–45 mg m^{-2}). Lower chlorophyll-*a* concentrations were found in October and November 2008 (range: 11–19 mg m^{-2}), which is explained by the dominance of the picoplankton (<2 μm) size fraction during those months and by the greater abundance of microphytoplankton (>20 μm) in February and May 2009 (range: 16–45 mg m^{-2}). The microphytoplankton community was dominated by *Skeletonema sp* during the study period with the exception of February 2009. *Skeletonema sp*. is usually significantly correlated with GPP in upwelling ecosystems (Montero et al., 2007). During this study the correlation between *Skeletonema* dominated phytoplankton community and GPP was also highly significant (without considering the February 2009 data, Spearman, $r=0.92$, $n=9$, $p<0.001$) indicating the importance of the *Skeletonema* genus to the overall productivity of Chilean coastal waters. During February 2009 the microplankton was mostly dominated by the mixotrophic dinoflagellate *Prorocentrum micans*. It has been argued that *P. micans* can exert a heavy grazing pressure upon diatoms (Yoo et al., 2009). It is possible that the low abundance of *Skeletonema* during February could be attributed to top down control of diatoms exerted by *P. micans*. The biomass normalized productivity (GPP/Chl-*a*) was higher during October 2008 and February 2009 reflecting a healthier physiological state of the microalgae community during the productive season (González et al., 2009).

Seasonal differences in GPP and phytoplankton biomass were also reflected in the total vertical flux of carbon (535.1 in August and a mean of 1336.6 ± 37 in October, February, and May). Although fecal pellets dominated the vertical carbon flux (20 ± 2 mg C m^{-2}), diatoms made a significant contribution to the downward transfer of organic carbon (13 mg C m^{-2}) in October 2008. The contribution of fecal pellets to vertical carbon fluxes reflects the importance of herbivorous pathways for food webs in the Reloncavi Fjord ecosystem. The observed increase in microzooplankton (dinoflagellates, ciliates) in October 2008 and February 2009, however, suggests that herbivorous pathways may not be the only route for carbon within the system. The concurrent increase in bacterial activity observed in spring and summer seems to indicate that carbon fluxes in Reloncavi Fjord are routed through a microbial food web coupled with a classical food chain and that the transfer of carbon to higher trophic levels is probably mediated by heterotrophic protists and mesozooplankton. Similar results have been reported by Vargas et al. (2008) for the Chiloé Interior Sea (41.5–43°). The contrasting set of conditions found in August 2008, with low rates of primary production and a greater contribution of small cells to autotrophic biomass, highlighted the importance of small-sized plankton and bacteria for the cycling and fluxes of carbon during the less productive winter months. Fecal pellet sedimentation was minimal during this period, which suggests that most of the locally-produced organic carbon is recycled within the microbial loop (Legendre and Le Fevre, 1995).

The strong and significant correlation between GPP and CR rates estimated during our study indicate a high degree of coupling between the synthesis of organic matter and its usage by the heterotrophic community. The balance between GPP and CR was close to unity during the study period ($GPP/CR=0.9\pm0.5$, $n=12$). Near the fjord head (St. P3) however, a predominance of heterotrophic activity was recorded during both the productive and the non-productive season. The high heterotrophic activity of the fjord head station is probably sustained by the input of allochthonous organic matter from the Cochamó River, which would allow the system to use more organic carbon than what is produced locally. The importance of river organic matter input to bacterial production was also reflected in St. P2, which is under the influence of the Puelo River. At this station winter bacterial

production (0.2 g C m^{-2} d^{-1}) was maintained despite the seasonal drop in phytoplankton production (0.1 ± g C m^{-2} d^{-1}). Similar results (describing the importance of river input of organic matter to coastal areas) have been reported for the Hudson River estuary New York by Findlay et al. (1991). Seasonal fluctuations in river water levels may also influence changes in primary production in marine coastal areas. Increased river discharge during the winter (June–August; León, 2005) may have reduce GPP in all our sampled stations because the increase sediment load reaching the fjord that have an impact on light attenuation values (Cole et al., 1992). Allochthonous carbon inputs, coupled with light constraints imposed on primary production in winter should favor a predominance of heterotrophic processes (Bukaveckas et al., 2002).

The productivity of bacterioplankton in most aquatic ecosystems depends mainly on the organic matter produced by the phytoplankton (Cole et al., 1988), although allochthonous terrestrial organic matter may also be used (Albright and McCrae, 1987). In this study, although we did not characterize the source of carbon utilized by bacterioplankton (i.e., allochthonous vs. in situ production), the significant correlation between GPP and BSP (Spearman, $r=0.68$, $p<0.05$, $n=9$) during the study period offers a strong indication that algal-derived carbon may be an important substrate for bacterial growth in the study zone.

Our estimates of BSP during the study period were similar to those observed in other ecosystems (Albright and McCrae, 1987; Duarte et al., 2005). During the productive season, however, the correspondence between leucine and thymidine estimates decreased. Differences between thymidine and leucine estimates have been interpreted as unbalanced growth by the bacterioplankton community since leucine measurements are associated with protein and thymidine with DNA synthesis (Chin-Leo and Kirchman, 1990; Gasol et al., 1998; Sherr et al., 2001). Thus, the imbalance that we observed during the productive season may reflect a shift towards protein synthesis during periods of more vigorous growth.

The significant correlation between CR and BSP (Spearman, $r=0.8$, $p<0.05$, $n=9$) indicates that bacterioplankton is responsible for a high proportion of CR in Reloncaví Fjord. Several authors, studying different ecosystems, have argued that bacterioplankton is able to process a significant proportion of organic matter produced by phytoplankton (Azam et al., 1983; Cole et al., 1988; Ducklow and Carlson, 1992; Turley et al., 2000; Cuevas et al., 2004; Montero et al., 2007). In this study, our results indicate that the utilization percentage of organic matter by bacterioplankton (BSP/GPP) varies between 8% and 59% (excluding winter data with % >100). Similar mean values were reported by Albright and McCrae (1987) for Howe Sound Fjord and by Ameryk et al. (2005) for the Gulf of Gdansk. Utilization percentages of organic matter by bacterioplankton over 100% (winter data) could be indicative that allochthonous carbon may be an important substrate for bacterial growth in months of low productivity.

It is generally accepted that grazing by phagotrophic protists, including flagellates and ciliates, is a major source of mortality for bacterioplankton (Pace, 1988; Sherr et al., 1992). In our study, the potential grazer community was composed of heterotrophic nanoflagellates (HNF), dinoflagellates, and ciliates (microzooplankton). The significant correlations found between these and the bacterioplankton biomass (Spearman, $r=0.7$, $p<0.05$, $n=12$) indicate that there is probably a strong top-down control of bacterial populations by their predators. This result, along with the close coupling showed by dinoflagellates and ciliates with HNF, Chl-*a*, and GPP, suggest that probably the microzooplankton; in agreement with (Vargas et al., 2008), may make a stronger link between the microbial and classic planktonic food webs in the study zone. In fact, several studies indicate that this group is one of the most important intermediaries between primary producers and copepods (Gifford, 1991; Calbet and Saiz, 2005) and constitutes a key component of the microbial food web (Azam et al., 1983; Sherr and Sherr, 2002).

The association between the microbial and the traditional food web allows "repackaging" the fixed carbon and offers an alternative route for the transfer of energy (Sherr and Sherr, 1988). Several authors (Legendre and Razzoulzadegan, 1995; Barber, 2007; Richardson and Jackson, 2007; Vargas et al., 2007) suggest that, in several aquatic ecosystems, different routes of carbon export may be associated and co-occur simultaneously, depending on the trophic links that are available within each ecosystem. Vargas et al. (2008) provide strong evidence that the food web structure in Reloncaví Fjord could be classified as multivorous, with both herbivorous and microbial grazing modes playing significant roles in carbon export. Finally, our results indicate that the bacterioplankton in fjord ecosystems are able to process a significant proportion of the organic carbon (allochthonous or local) that enters these systems, possibly offering a permanent, fundamental path for the transfer of energy within the carbon flux.

Acknowledgements

We acknowledge funding from FIP project 2007-21 and from the COPAS Sur Austral (PFB-31/2007) research program.

References

Acha, E.M., Mianzan, H.W., Guerrero, R.A., Favero, M., Bava, J., 2004. Marine fronts at the continental shelves of austral South America: physical and ecological processes. J. Mar. Syst. 44, 83–105.

Albright, L.J., McCrae, S.K., 1987. Annual bacterioplankton biomasses and productivities in a temperate west coast Canadian fjord. Appl. Environ. Microbiol. 53 (6), 1277–1285.

Ameryk, A., Podgórska, B., Witek, Z., 2005. The dependence between bacterial production and environmental conditions in the Gulf of Gdansk. Oceanologia 47, 27–45.

Aristegui, J., Harrison, W.G., 2002. Decoupling of primary production and community respiration in the ocean: implications for regional carbon studies. Mar. Ecol. Prog. Ser. 29, 199–209.

Azam, F., Fenchel, T., Field, J.G., Gray, J.S., Meyer-Reil, L.A., Thingstad, F., 1983. The ecological role of water-column microbes in the sea. Mar. Ecol. Prog. Ser. 10, 257–263.

Barber, R., 2007. Picoplankton do some heavy lifting. Science 315, 777–778.

Børsheim, K.Y., Bratbak, G., 1987. Cell volume to cell carbon conversion factors for a bacterivorous *Monas sp.* enriched from sea water. Mar. Ecol. Prog. Ser. 36, 171–175.

Bukaveckas, P.A, Williams, J.J., Hendricks, S.P., 2002. Factors regulating autotrophy and heterotrophy in the main channel and an embayment of a large river impoundment. Aquat. Ecol. 36, 355–369.

Burrell, D.C., 1988. Carbon flow in fjords. Oceanogr. Mar. Biol. Annu. Rev., 143–226.

Button, D.K., 1984. Evidence for a terpene-based food chain in the Gulf of Alaska. Appl. Environ. Microbiol. 48, 1004–1011.

Calbet, A., Landry, M.R., 2004. Phytoplankton growth, microzooplankton grazing, and carbon cycling in marine systems. Limnol. Oceanogr. 49, 51–57.

Calbet, A., Saiz, E., 2005. The ciliate-copepod link in marine ecosystems. Aquat. Microb. Ecol. 38, 157–167.

Chaigneau, A., Pizarro, O., 2005. Mean surface circulation and mesoscale turbulent flow characteristics in the eastern South Pacific from satellite tracked drifters. J. Geophys. Res. vol. 110, C05014. doi:10.1029/2004JC002628 2005.

Chin-Leo, G., Kirchman, D.L., 1990. Unbalanced growth in the natural assemblages of marine bacterioplankton. Mar. Ecol. Prog. Ser. 63, 1–8.

Cole, J.J., Findlay, S., Pace, M.L., 1988. Bacterial production in fresh and saltwater ecosystems: a cross-system overview. Mar. Ecol. Prog. Ser. 43, 1–10.

Cole, J.J., Caraco, N.F., Peierls, B.L., 1992. Can phytoplankton maintain a positive carbon balance in a turbid, freshwater, tidal estuary? Limnol. Oceanogr. 37 1608–1617.

Collins, A.K., Allen, S.E., Pawlowicz, R., 2009. The role of wind in determining the timing of the spring bloom in the Strait of Georgia. Can. J. Fish. Aquat. Sci. 66, 1597–1616.

Cuevas, L.A., Daneri, G., Jacob, B., Montero, P., 2004. Microbial abundance and activity in the seasonal upwelling area off Concepción (~36°S), central Chile: a comparison of upwelling and non-upwelling conditions. Deep-Sea Res. II 51, 2427–2440.

Czypionka, T., Vargas, C., Silva, N., Daneri, G., González, H.E., Iriarte, J.L.. On the prevalence of mixotrophic plankton in the fjord region of southern Chile: a call for the consideration of mixotrophy in ecosystem analysis of fjords and coastal embayment. Cont. Shelf Res., this issue.

Duarte, C.M., Agustí, S., Vaqué, D., Agawin, N.S.R., Felipe, J., Casamayor, E.O., Gasol, J.M., 2005. Experimental test of bacteria–phytoplankton coupling in the Southern Ocean. Limnol. Oceanogr. 50, 1844–1854.

Ducklow, H.W., Carlson, C.A., 1992. Oceanic bacterial productivity. Adv. Microb. Ecol. 12, 113–181.

Edler, L., 1979. Recommendations for marine biological studies in the Baltic Sea. Balt. Mar. Biol. Publ. 5, 1–38.

Findlay, S., Pace, M.L., Lints, D., Cole, J.J., Caraco, N.F., Peierls, B., 1991. Weak coupling of bacteria and algal production in a heterotrophic ecosystem: the Hudson River estuary. Limnol. Oceanogr. 36, 268–278.

Fuhrman, J.A., Azam, F., 1982. Thymidine incorporation as a measure of heterotrophic bacterioplankton production in marine surface waters: evaluation and field results. Mar. Biol. 66, 109–120.

Gasol, J.M., Doval, M.D., Pinhassi, J., Calderón-Paz, J.I., Guixa-Boixareu, N., Vaqué, D., Pedrós-Alió, C., 1998. Diel variations in bacterial heterotrophic activity and growth in the northwestern Mediterranean Sea. Mar. Ecol. Prog. Ser. 164, 107–124.

Gifford, D.J., 1991. The protozoan–metazoan trophic link in pelagic ecosystems. J. Protozool. 38, 81–86.

Goebel, N.L., Wing, S.R., Boyd, P.W., 2005. A mechanism for onset of diatom blooms in a fjord with persistent salinity stratification. Estuar. Coast. Shelf Sci. 64, 546–560.

González, H.E., Ortiz, V., Sobarzo, M., 2000. The role of faecal material in the particulate organic carbon flux in the northern Humboldt Current, Chile (23°S), before and during the 1997–1998 El Niño. J. Plankton Res. 22, 499–529.

González, H.E., Daneri, G., Iriarte, J.L., Yaninicelli, B., Menschel, E., Barría, C., Pantoja, S., Lizárraga, L., 2009. Carbon fluxes within the epipelagic zone of the Humboldt Current System off Chile: the significance of euphasiids and diatoms as key functional groups for the biological pump. Prog. Oceanogr. 83, 217–227.

González, H.E., Castro, L., Daneri, G., Iriarte, J.L., Silva, N., Vargas, C., Giesecke, R., Sánchez, N. . Seasonal plankton variability in Chilean Patagonia Fjords: carbon flow through the pelagic food web of the Aysen Fjord and plankton dynamics in the Moraleda Channel basin. Cont. Shelf Res., this issue.

Hass, L., 1982. Improved epifluorescence microscopy for observing planktonic micro-organisms. Ann. Inst. Oceanogr. 58, 261–266.

Iriarte, J.L., Gonzalez, H.E., 2008. Phytoplankton bloom ecology of the inner Sea of Chiloé, Southern Chile. Nova Hedwigia 133, 67–79 Beiheft.

Iriarte, J.L., Gonzalez, H.E., Liu, K.K., Rivas, C., Valenzuela, C., 2007. Spatial and temporal variability of chlorophyll and primary productivity in surface waters of southern Chile (41.5–43°S). Estuar. Coast. Shelf Sci. 74, 471–480.

Lee, S., Fuhrman, J., 1987. Relationship between biovolume and biomass of naturally-derived marine bacterioplankton. Appl. Environ. Microbiol. 53, 1298–1303.

Legendre, L., Le Fevre, J., 1995. Microbial food webs and the export of biogenic carbon in oceans. Aquat. Microb. Ecol. 9, 69–77.

Legendre, L., Razzoulzadegan, F., 1995. Plankton and nutrient dynamics in marine waters. Ophelia 41, 153–172.

Legendre, L., Razzoulzadegan, F., 1996. Food-web mediated export of biogenic carbon in oceans: hydrodynamic control. Mar. Ecol. Prog. Ser. 145, 179–193.

Legendre, L., Rivkin, R.B., 2002. Fluxes of carbon in the upper ocean: regulations by food-webs control nodes. Mar. Ecol. Prog. Ser. 242, 95–109.

Legendre, L., Rivkin, R.B., 2008. Planktonic food webs: microbial hub approach. Mar. Ecol. Prog. Ser. 365, 289–309.

León, J.E., 2005. Influencia del caudal del río Puelo sobre la salinidad y concentración de oxígeno disuelto en el Estuario de Reloncaví, Llanquihue, Chile. Master's thesis, Universidad Austral de Chile, 74 pp.

McManus, G., Peterson, W.T., 1988. Bacterioplankton production in the nearshore zone during upwelling off central Chile. Mar. Ecol. Prog. Ser. 43, 11–17.

Montero, P., Daneri, G., Cuevas, L.A., González, H.E., Jacob, B., Lizárraga, L., Menschel, E., 2007. Productivity cycles in the coastal upwelling area of Concepción: the importance of diatoms and bacteria in the flux of organic carbon. Prog. Oceanogr. 75 (3), 518–530.

Newell, S.Y., Christian, R.R., 1981. Frequency of dividing cells as an estimator of bacterial productivity. Appl. Environ. Microbiol. 42, 23–31.

Pace, M.L., 1988. Bacterial mortality and the fate of bacterial production. Hydrobiologia 159, 41–50.

Parsons, T.R., Maita, R., Lalli, C.M., 1984. Counting, media and preservatives. A manual of chemical and biological methods for seawater analysis. Pergamon Press, Toronto (pp. 1–163).

Pickard, G.L., 1971. Some physical oceanographic features of inlets of Chile. J. Fish. Res. Board Can. 28, 1077–1106.

Pizarro, G., Iriarte, J.L., Montecino, V., Blanco, J.L., Guzmán, L., 2000. Distribución de la biomasa fitoplanctónica y productividad primaria máxima de fiordos y canales australes (47–50°S) en octubre 1996. Cienc. Tecnol. Mar 23, 25–48.

Pizarro, G., Astoreca, R., Montecino, V., Paredes, M.A., Alarcón, G., Uribe, P., Guzmán, L., 2005. Patrones espaciales de la abundancia de la clorofila, su relación con la productividad primaria y la estructura de tamaños del fitoplancton en Julio y Noviembre de 2001 en la región de Aysén (43–56°S). Cienc. Tecnol. Mar 28 (2), 27–42.

Porter, K., Feig, Y., 1980. The use of DAPI for identifying and counting aquatic microflora. Limnol. Oceanogr. 25, 943–948.

Richardson, T.L., Jackson, G.A., 2007. Small phytoplankton and carbon export from the surface ocean. Science 315, 838–840.

Rivkin, R.B., Legendre, L., 2001. Biogenic carbon cycling in the upper ocean: effects of microbial respiration. Science 291, 2398–2400.

Rojas, N., Silva, S., 2005. Early diagenesis and vertical distribution of organic carbon and total nitrogen in recent sediments from southern Chilean fjords (Boca del Guafo to Pulluche Channel). Invest. Mar. 33, 183–194.

Sherr, E.B., Sherr, B.F., 1988. Role of microbes in pelagic food webs: a revised concept. Limnol. Oceanogr. 33, 1225–1227.

Sherr, E.B., Sherr, B.F., 2002. Significance of predation by protists in aquatic microbial food webs. Antonie van Leeuwenhoek 81, 293–308.

Sherr, E.B., Sherr, B.F., McDaniel, J., 1992. Effect of protistan grazing on the frequency of dividing cells in bacterioplankton assemblages. Appl. Environ. Microbiol. 58, 2381–2385.

Sherr, E.B., Sherr, B.F., Cowles, T.J., 2001. Mesoscale variability in bacterial activity in the Northeast Pacific Ocean off Oregon, USA. Aquat. Microb. Ecol. 25, 21–30.

Silva, N., 2008. Dissolved oxygen, pH, and nutrients in the austral Chilean channels and fjords. In: Silva, N., Palma, S. (Eds.), Progress in the oceanographic Knowledge of Chilean interior waters. Comité Oceanográfico Nacional – Pontificia Universidad Católica de Valparaíso, Valparaíso, pp. 37–43 from Puerto Montt to Cape Horn.

Silva, N., Prego, R., 2002. Carbon and nitrogen spatial segregation and stoichiometry in the surface sediments of southern Chilean inlets (41°–56′S). Estuarine Cont. Shelf Sci. 55, 763–775.

Silva, N., Calvete, M., Sievers, H., 1997. Características oceanográficas físicas y químicas de canales australes chilenos entre Puerto Montt y Laguna san Rafael (Crucero CIMAR-Fiordo 1). Cienc. Tecnol. Mar 20, 23–106.

Silva, N., Calvete, C., Sievers, H., 1998. Masas de agua y circulación general para algunos canales australes entre Puerto Montt y Laguna San Rafael, Chile (Crucero Cimar-Fiordo 1). Cienc. Tecnol. Mar 20, 17–48.

Simon, M., Azam, F., 1989. Protein content and protein synthesis rates of planktonic marine bacteria. Mar. Ecol. Prog. Ser. 51, 201–213.

Strickland, J.D.H., 1960. Measuring the production of marine phytoplankton. Bull. Fish. Res. Board Can. 122, 1–72.

Strickland, J.D.H., Parsons, T.R., 1968. Determination of reactive nitrite, in: A Practical Handbook of Seawater Analysis. Bull. Fish. Res. Board Can. 167, 71–75.

Sun, J., Liu, D., 2003. Geometric models for calculating cell biovolume and surface area for phytoplankton. J. Plankton Res. 25 (2), 1331–1346.

Sverdrup, H.U., 1953. On conditions for the vernal blooming of phytoplankton. J. Cons. Int. Explor. Mer. 18, 287–295.

Turley, C.M., Bianchi, M., Christiaki, U., Conan, P., Harris, J.R.W., Psarra, S., Ruddy, G., Stutt, E.D., Tselepides, A., Van Wambeke, F., 2000. Relationship between primary producers and bacteria in an ologotrophic sea: the Mediterranean and biogeochemical implications. Mar. Ecol. Prog. Ser. 193, 11–18.

Utermöhl, H., 1958. Zur Vervollkommnung der quantitativen phytoplankton methodik. Mitt. Int. Ver. Theor. Angew. Limnol. 9, 1–39.

Vargas, C.A., Martínez, R., Cuevas, L.A., Pavez, M.A., Cartes, C., González, H.E., Escribano, R., Daneri, G., 2007. The relative importance of microbial and classical food webs in a highly productive coastal upwelling area. Limnol. Oceanogr. 52, 1495–1510.

Vargas, C.A., Martínez, R., González, H.E., Silva, N., 2008. Contrasting trophic interactions of microbial and copepod communities in a fjord ecosystem, Chilean Patagonia. Aquat. Microb. Ecol. 53, 227–242.

Verity, P., Langdon, C., 1984. Relationships between lorica volume, carbon, nitrogen, and ATP content of tintinnids in Narragansett Bay. J. Plankton Res. 6, 859–868.

Wicks, R.J., Robarts, R.D., 1987. The extraction and purification of DNA labelled with [methyl-3H] thymidine in aquatic bacterial production studies. J. Plankton Res. 9 (6), 1159–1166.

Williams, P.J.LeB, 1998. The balance of plankton respiration and the photosynthesis in the open ocean. Nature 394, 55–57.

Williams, P.J.LeB., Robertson, J.E, 1991. Overall planktonic oxygen and carbon dioxide metabolism: the problem of reconciling observations and calculations of photosynthetic quotients. J. Plankton Res. 13 (1), 153–169.

Yoo, Y.D., Jeong, H.J., Kim, M.S., Kang, N.M., Song, J.K., Shin, W., Kim, K.Y., Lee, K., 2009. Feeding by phototrophic red-tide dinoflagellates on the ubiquitous marine diatom *Skeletonema costatum*. J. Eukaryot. Microbiol. 56 (5), 413–420.